# Electronic Structure of the 1-(Benzoyloxy)ethyl Radical#

Nozomu UCHIDA, Tomoo SHIOMI, Kiyokazu IMAI, and Hiroshi TATEWAKI*,†
Department of Chemistry, Nagaoka University of Technology, Kamitomioka 1603-1, Nagaoka 940-21
† Computation Center, Nagoya City University, Mizuho-ku, Nagoya 467

(Received March 23, 1993)

In the polymerization of vinyl benzoate, the tacticity of the obtained polymer is changed toward less isotactic by UV irradiation. To explain this phenomenon, it was assumed that the growing terminal of the polymer was excited by UV irradiation and that the coplanarity of the vinyl benzoates was broken. It was thus naturally concluded that the existence of a twisted radical reduced the isotacticity. To examine the above assumption, the electronic structures of the ground and excited states of 1-(benzoyloxy)ethyl radical ($CH_3\dot{C}HOCOC_6H_5$) were studied as a model of the growing terminal of the polymer by ab initio SCF and CI calculations. The present calculation, however, showed that the planer structure was stable in both the ground and excited states.

Poly(vinyl alcohol) (PVA) is one of the most important materials in the polymer industry. The properties of PVA are strongly influenced by its stereoregularity. However, PVA can be obtained only through radical polymerization of vinyl esters followed by saponification of the products. It has been generally known that it is hard to control the stereoregularity in the radical polymerization process.

The stereoregularity of polymers is represented by tacticity. The case in which D- and L-type carbons are lined up alternatively is called syndiotactic; the case in which either the D- or L-type asymmetric carbons are lined up in the polymer chain is called isotactic; and the randomly lined up case is called atactic (Fig. 1). The products of radical polymerization are usually either atactic or slightly syndiotactic.

To control the stereoregularity of PVA, several synthesis conditions, such as the solvents and structure of the starting materials, have been examined.[1,2] It was reported that the stereoregularity of poly(vinyl ester), which is the precursor of PVA, was strongly affected by group R of the starting vinyl esters ($CH_2$=CHOCOR). When group R was an alkyl, the syndiotacticity of the product increased with the size of R.[3—5] On the other hand, when R was a phenyl, and coplanarity existed between the phenyl group and the carbonyl group, the product became slightly isotactic.[6] When the coplanarity was broken, i.e., in case that the R was the ortho substituted phenyl group, the isotacticity of the product was reduced.[7]

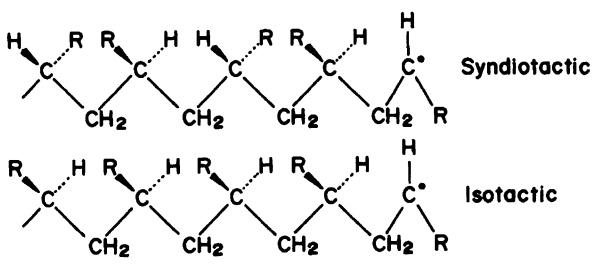


Fig. 1. Expression of the stereoregularity of polymers.

Recently, in case of vinyl benzoates (VBz), where phenyl and carbonyl groups are in one plane, it was observed that the isotacticity of the product was reduced by ultraviolet irradiation (either 352 nm=3.52 eV with a half-peak width of 0.40 eV or 253.7 nm=4.89 eV (line spectrum)) during the polymerization.[8] To explain this phenomenon, it was assumed that 1) the growing terminal radical of the polymer was excited by UV irradiation, 2) the coplanarity was broken in the excited states, and 3) the excited states either directly or indirectly contributed to the polymerization. In this explanation, the interactions between the growing terminal and the solvent are disregarded; the explanation thus remains in the category of the mono-molecular process.

The purpose of the present study was to examine assumptions 1) and 2) based on the theoretical calculations. The 1-(benzoyloxy)ethyl radical ($CH_3\dot{C}HOCOC_6H_5$) was selected as a model molecule which simulates the growing terminal radical of the polymer. The total energies of the ground and excited states were calculated as a function of the angle between the phenyl and carbonyl groups on the basis of an ab initio self-consistent field (SCF), a Tamm–Dankoff (TD)-like configuration interaction (CI) calculations, and two other types of CI calculations with single and double excitations from multi-reference configuration state functions (MRCSF).

We close the introduction with an interesting experimental fact that contrary to the case of irradiation of a coplanarity complex, irradiation had no effect on the polymerization of vinyl *o*-chlorobenzoate, in which the phenyl group was twisted against the carbonyl group.[8]

## Model Molecule and Basis Set

The geometry of the model molecule, the 1-(benzoyloxy)ethyl radical, was determined by referring to the geometry of the constituent molecular units. The structure of the model molecule is shown in Fig. 2, and the geometrical data are summarized in Table 1. On a real polymer system, the remaining part is connected to C16

#This paper is dedicated to the memory of the late Professor Hiroshi Kato.

Table 1. Geometry Data of the Model Radical, $CH_3\dot{C}HOCOC_6H_5$

| Bond length (Å) | | Ref. | Bond angle (degree) | | Ref. | Torsion angle (degree) | | Ref. |
|---|---|---|---|---|---|---|---|---|
| C1–O2 | 1.36 | a | O3–C1–O2 | 124.0 | c | H19–C16–C15–H18 | 120.0 | d |
| C1–O3 | 1.24 | a | O4–C1–C2 | 113.0 | a | H20–C16–C15–H18 | 240.0 | d |
| C1–C4 | 1.48 | a | C5–C4–C1 | 122.0 | a | | | |
| C4–C5 | 1.39 | a | C6–C5–C4 | 118.0 | a | | | |
| C5–C6 | 1.42 | a | C7–C6–C5 | 123.0 | a | | | |
| C6–C7 | 1.36 | a | C8–C7–C6 | 118.0 | a | | | |
| C4–C8 | 1.39 | a | C9–C8–C4 | 120.0 | a | | | |
| C8–C9 | 1.41 | a | C8–C9–C7 | 122.0 | a | | | |
| C7–C9 | 1.37 | a | H10–C5–C4 | 121.0 | e | | | |
| C–H in phenyl group | | | H11–C6–C5 | 118.0 | e | | | |
| | 1.084 | b | H12–C7–C6 | 121.0 | e | | | |
| O2–C15 | 1.46 | c | H13–C9–C8 | 119.0 | e | | | |
| C15–C16 | 1.54 | d | H14–C8–C4 | 120.0 | e | | | |
| C15–H17 | 1.09 | d | C15–O2–C1 | 113.0 | c | | | |
| C16–H18, 19, 20 | 1.09 | d | C16–C15–O2 | 120.0 | f | | | |
| | | | H17–C15–O2 | 120.0 | f | | | |
| | | | H18, 19, 20–C16–C15 | 109.5 | d | | | |

References: a) benzoic acid,[9] b) benzene,[9] c) methyl acetate,[9] d) ethanol,[9] e) a half of the outer C–C–C angle of the ring, f) angle of $sp^2$ hybridized orbital.

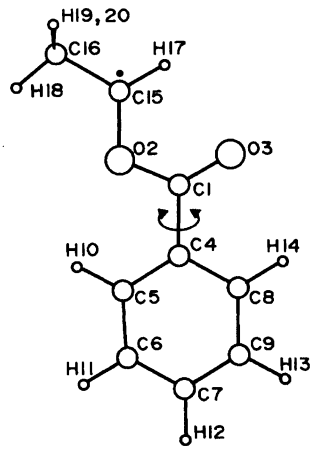


Fig. 2. Structure of the model radical $CH_3\dot{C}HOCOC_6H_5$.

where H18 is substituted with an asymmetric carbon atom.

To investigate the potential curve of the rotation, the bond C1–C4 was twisted and the torsion angles between the phenyl and carbonyl groups were set to 0°, 15°, and 30°. Since this molecule has a $C_s$ symmetry at a torsion angle of 0°, the clockwise and anticlockwise twistings have equivalent meanings. We used the $C_1$ symmetry even at 0°, since we intended to treat a molecule having a torsion angle of 0° to 30° using the same terminology and with the same accuracy.

In the excited states, the molecular structure can change drastically from that of the ground state; the coplanarity can be broken not only by torsion, but also by bending. In this paper, however, we discuss only the twisting of the C1–C4 bond on the basis of the experimental result.[7]

The basis set for the molecular integrals is that of a split-valence Gaussian-type, MIDI4:[10] (421/31) for C and O and (31) for H.

An SCF calculation was first carried out for the $^2$A ground state.

Secondly, by using the MO's of $^2$A, a one-electron excitation CI calculation (called Tamm–Dankoff (TD)-like CI) was performed in order to obtain the electronic states of the $^2$A state and the $^4$A state in SCF-level approximations.

Thirdly, using the results of the TD-like CI, we performed two larger CI calculations, one of which was a multiconfiguration SCF-like. Details concerning the CI calculations are given in the next section.

## Calculations

**SCF-MO Calculation.** There are 117 molecular orbitals (MOs) for the molecule. Thirty nine of them are doubly occupied, and one of them is singly occupied in the $^2$A ground state,

$$\{(1a)^2 \ldots\ldots (38a)^2\}(39a)(40a)^2 \qquad {}^2A \qquad (1)$$

At a torsion angle of 0°, this is equivalent to

$$\{(1a'(\sigma))^2 \ldots (33a'(\sigma))\}\times \{(1a''(\pi))^2 \ldots (5a''(\pi))^2\}(6a''(\pi))(7a''(\pi))^2 \quad {}^2A'' \qquad (2)$$

All of the occupied $\pi$-orbitals, as well as the occupied $\sigma$- and virtual orbitals, which will play an important role in the CI calculations, are collected in Table 2. Orbital 39a is almost at a $p_z$ of C15, which is consistent with the ordinary expectations concerning the localization of a radical electron. We found that the SCF MOs for the ground state at torsion angles of 0° and 30° resemble each other, suggesting that the characteristics of the orbitals ($\sigma$ and $\pi$) were fairly well preserved through

Table 2. Important SCF Orbitals of the Torsion Angle 0°

| Orbital | MO energy (a.u.) | Character[a] | | TE[c] = −494.96979 a.u. | | |
|---|---|---|---|---|---|---|
| 25($\pi$): | −0.6483 | [+0.28($2p_{zi}$[b])C1) | +0.14($2p_{zo}$[b])C1) | +0.46($2p_{zi}$O2) | | |
| | | +0.32($2p_{zo}$O2) | +0.21($2p_{zi}$O3) | +0.13($2p_{zo}$O3)] | | |
| 29a($\pi$): | −0.5795 | [−0.43($2p_{zi}$C16) | −0.21($2p_{zo}$C16) | +0.31($1s_i$H19) | −0.31($1s_i$H20)] | |
| 30a($\sigma$): | −0.5774 | [−0.23($2p_{yi}$O2) | −0.17($2p_{yo}$O2) | −0.20($2p_{yi}$O3) | −0.13($2p_{yo}$O3) | +0.29($2p_{yi}$C16) |
| | | +0.16($2p_{yo}$C16) | −0.27($1s_i$H18)] | | | |
| 32a($\pi$): | −0.5265 | [+0.23($2p_{zi}$O2) | +0.18($2p_{zo}$O2) | −0.22($2p_{zi}$C4) | −0.15($2p_{zo}$C4) | −0.19($2p_{zi}$C5) |
| | | −0.19($2p_{zi}$C6) | −0.12($2p_{zo}$C6) | −0.20($2p_{zi}$C7) | −0.11($2p_{zo}$C7) | −0.20($2p_{zi}$C8) |
| | | −0.11($2p_{zo}$C8) | −0.20($2p_{zi}$C9) | −0.12($2p_{zo}$C9)] | | |
| 33a($\sigma$): | −0.5230 | [−0.20($2p_{yi}$O2) | −0.17($2p_{yo}$O2) | +0.23($2p_{xi}$O3) | +0.15($2p_{xi}$O3) | +0.10($2p_{xi}$C5) |
| | | +0.12($2p_{yi}$C5) | −0.15($2p_{xi}$C6) | −0.12($2p_{yi}$C6) | +0.15($2p_{xi}$C7) | +0.16($2p_{yi}$C7) |
| | | +0.13($2p_{xi}$C8) | +0.20($2p_{yi}$C8) | −0.16($2p_{xi}$C9) | −0.17($2p_{yi}$C9) | −0.20($1s_i$H12) |
| | | +0.17($1s_i$H13)] | | | | |
| 34a($\sigma$): | −0.5206 | [+0.15($2p_{yi}$O2) | +0.12($2p_{yo}$O2) | +0.16($2p_{yi}$C7) | +0.14($2p_{yi}$C8) | +0.27($2p_{xi}$C15) |
| | | −0.15($2p_{yi}$C15) | +0.12($2p_{xo}$C15) | −0.26($2p_{xi}$C16) | +0.12($2p_{yi}$C16) | −0.12($2p_{xo}$C16) |
| | | −0.24($1s_i$H17) | −0.20($1s_i$H18)] | | | |
| 36a($\pi$): | −0.4833 | [+0.20($2p_{zi}$C1) | +0.13($2p_{zo}$C1) | −0.32($2p_{zi}$O2) | −0.29($2p_{zo}$O2) | +0.43($2p_{zi}$O3) |
| | | +0.34($2p_{zo}$O3)] | | | | |
| 37a($\sigma$): | −0.4540 | [−0.15($2s_o$O2) | +0.21($2p_{xi}$O2) | +0.21($2p_{xo}$O2) | +0.42($2p_{xi}$O3) | +0.34($2p_{yi}$O3) |
| | | +0.32($2p_{xo}$O3) | +0.25($2p_{yo}$O3) | +0.21($2p_{xi}$C4) | +0.20($2p_{yi}$C4) | +0.26($2p_{yo}$C4)] |
| 38a($\pi$): | −0.3667 | [−0.33($2p_{zi}$C4) | −0.30($2p_{zo}$C4) | −0.19($2p_{zi}$C5) | −0.13($2p_{zo}$C5) | +0.31($2p_{zi}$C7) |
| | | +0.24($2p_{zo}$C7) | +0.19($2p_{zi}$C9) | +0.14($2p_{zo}$C9)] | | |
| 39a($\pi$): | −0.3618 | [−0.66($2p_{zi}$C15) | −0.54($2p_{zo}$C15)] | | | |
| 40a($\pi$): | −0.3435 | [+0.26($2p_{zi}$C5) | +0.22($2p_{zo}$C5) | +0.30($2p_{zi}$C6) | +0.26($2p_{zo}$C6) | −0.30($2p_{zi}$C8) |
| | | −0.24($2p_{zo}$C8) | −0.27($2p_{zi}$C9) | −0.23($2p_{zo}$C9)] | | |
| 41a($\sigma$): | −0.1131 | [−0.16($2s_i$O2) | −0.75($2s_o$O2) | −0.34($2p_{yi}$O2) | −0.23($2p_{xo}$O2) | −0.54($2p_{yo}$O2) |
| | | −0.14($1s_i$C15) | +0.41($2s_i$C15) | +1.22($2s_o$C15) | −0.22($2p_{xi}$C15) | −0.36($2p_{yi}$C15) |
| | | −0.46($2p_{xo}$C15) | −0.54($2p_{yo}$C15)] | | | |
| 42a($\pi$): | −0.0874 | [+0.43($2p_{zi}$C1) | +0.47($2p_{zo}$C1) | −0.30($2p_{zi}$O3) | −0.39($2p_{zo}$O3) | +0.14($2p_{zi}$C4) |
| | | +0.22($2p_{zo}$C4) | −0.18($2p_{zi}$C5) | −0.27($2p_{zo}$C5) | +0.18($2p_{zi}$C7) | +0.26($2p_{zo}$C7) |
| | | −0.17($2p_{zi}$C8) | −0.28($2p_{zo}$C8)] | | | |
| 45a($\pi$): | 0.0213 | [+0.28($2p_{zi}$C5) | +0.56($2p_{zo}$C5) | −0.29($2p_{zi}$C6) | −0.56($2p_{zo}$C6) | −0.27($2p_{zi}$C8) |
| | | −0.52($2p_{zo}$C8) | +0.28($2p_{zi}$C9) | +0.51($2p_{zo}$C9)] | | |
| 46a($\sigma$): | 0.0328 | [−0.76($1s_o$H10) | +0.28($2s_i$C15) | +1.10($2s_o$C15) | +0.48($2p_{xi}$C15) | +1.32($2p_{xo}$C15) |
| | | +0.22($2p_{yo}$C15) | −0.76($2s_o$C16) | +0.34($2p_{xi}$C16) | +1.65($2p_{xo}$C16) | −0.16($2p_{yo}$C16) |
| | | −0.97($1s_o$H18)] | | | | |
| 47a($\pi$): | 0.0398 | [−1.72($1s_o$H19) | −1.72($1s_o$H20)] | | | |
| 48a($\sigma$): | 0.0547 | [−0.90($1s_o$H10) | −1.21($1s_o$H18) | +1.07($1s_o$H19) | +1.07($1s_o$H20)] | |
| 49a($\pi$): | 0.0822 | [+0.33($2p_{zi}$C1) | +0.60($2p_{zo}$C1) | −0.34($2p_{zi}$C4) | −0.07($2p_{zo}$C4) | +0.16($2p_{zi}$C6) |
| | | +0.32($2p_{zo}$C6) | −0.27($2p_{zi}$C7) | −0.58($2p_{zo}$C7) | +0.15($2p_{zi}$C9) | +0.32($2p_{zo}$C9)] |
| 56a($\pi$): | 0.2447 | [+0.29($2p_{zi}$C4) | +0.87($2p_{zo}$C4) | −0.20($2p_{zi}$C5) | −0.77($2p_{zo}$C5) | +0.22($2p_{zi}$C6) |
| | | +0.78($2p_{zo}$C6) | −0.25($2p_{zi}$C7) | −0.85($2p_{zo}$C7) | −0.22($2p_{zi}$C8) | −0.80($2p_{zo}$C8) |
| | | +0.24($2p_{zi}$C9) | +0.82($2p_{zo}$C9)] | | | |
| 57a($\sigma$): | 0.2849 | [−0.17($2s_i$C1) | −1.12($2s_o$C1) | −0.22($2p_{xi}$C1) | −1.26($2p_{xo}$C1) | +1.77($2p_{yo}$C1) |
| | | −0.12($2s_i$C8) | −0.12($2p_{xi}$C8) | +0.37($2p_{xo}$C8) | +0.69($2p_{yo}$C8) | +0.12($2s_i$C15) |
| | | +0.36($2s_o$C15) | +0.32($2p_{xi}$C15) | −0.44($2p_{xo}$C15) | −0.49($2p_{yo}$C15) | |

a) The atoms having large gross atomic population are given. The atomic orbitals having major contribution are in parentheses. b) i and o mean the inner and outer parts of the sprit valence atomic orbital, respectively. c) TE means total SCF energy.

rotation up to 30°.

Figure 3 shows the total energy curve of the ground state obtained by SCF calculations as a function of the torsion angle. The potential curve appears to be very shallow, and is thus consistent with a very slow change in the characteristics of the orbitals discussed above.

**TD-Like CI Calculation.** In this CI calculation, only the CSF's arising from one-electron excitation from the reference configuration (1) were used for both $^2$A and $^4$A. The occupied SCF-MOs from No. 1 to 11 were treated as a frozen core, since there was a large MO energy gap of almost 10 a.u. between the 11-th and 12-th MOs, and the deformation of these orbitals was expected to be fairly small when the molecule was excited. The occupied MOs from No. 12 to 40 for $^2$A were treated as valence orbitals, and all of the virtual orbitals were treated as semi-valence orbitals, in which one-electron excitation is permitted.

The solutions up to the eighth were calculated for the $^2$A and $^4$A states. The total energies vs. the ro-

Table 3. TD-CI Wave Functions of TD-like CI

| $^2$A states | | | | | $\Delta E$ (eV) $\{E-E(1^2\text{A } 0°)\}$[a] |
|---|---|---|---|---|---|
| Torsion angle 0° | | | | | |
| $\Psi$ ($1^2$A) = | 0.99(CSF1) | +··· | | | 0.000 |
| $\Psi$ ($2^2$A) = | 0.71(CSF46) | +0.51(CSF32) | −0.32(CSF38) | +··· | 3.536 |
| $\Psi$ ($3^2$A) = | −0.77(CSF44) | +0.47(CSF52) | −0.27(CSF34) | +··· | 4.834 |
| $\Psi$ ($4^2$A) = | −0.55(CSF32) | +0.50(CSF46) | −0.47(CSF18) | +··· | 5.014 |
| $\Psi$ ($5^2$A) = | 0.55(CSF18) | +0.44(CSF39) | +0.40(CSF46) | +0.39(CSF38) | |
| | −0.30(CSF32) | +··· | | | 5.475 |
| $\Psi$ ($6^2$A) = | 0.87(CSF24) | +0.30(CSF54) | +0.22(CSF28) | +··· | 5.493 |
| $\Psi$ ($7^2$A) = | −0.91(CSF23) | +0.21(CSF27) | +··· | | 6.237 |
| $\Psi$ ($8^2$A) = | 0.76(CSF43) | −0.47(CSF33) | −0.42(CSF51) | +··· | 6.264 |
| Torsion angle 15° | | | | | |
| $\Psi$ ($1^2$A) = | 0.99(CSF1) | +··· | | | 0.022 |
| $\Psi$ ($2^2$A) = | 0.72(CSF46) | +0.50(CSF32) | +0.32(CSF38) | +··· | 3.568 |
| $\Psi$ ($3^2$A) = | 0.75(CSF44) | +0.44(CSF52) | +0.27(CSF34) | +··· | 4.894 |
| $\Psi$ ($4^2$A) = | 0.54(CSF32) | −0.47(CSF46) | −0.47(CSF18) | +··· | 5.049 |
| $\Psi$ ($5^2$A) = | −0.51(CSF24) | +0.48(CSF18) | −0.35(CSF39) | −0.31(CSF46) | |
| | −0.27(CSF38) | +0.24(CSF32) | +··· | | 5.473 |
| $\Psi$ ($6^2$A) = | −0.70(CSF24) | +0.27(CSF46) | −0.26(CSF18) | −0.26(CSF38) | |
| | −0.24(CSF54) | +··· | | | 5.546 |
| $\Psi$ ($7^2$A) = | −0.80(CSF23) | +0.32(CSF43) | +··· | | 6.233 |
| $\Psi$ ($8^2$A) = | −0.67(CSF43) | +0.44(CSF33) | −0.37(CSF51) | −0.36(CSF23) +··· | 6.333 |
| Torsion angle 30° | | | | | |
| $\Psi$ ($1^2$A) = | 0.99(CSF1) | +··· | | | 0.086 |
| $\Psi$ ($2^2$A) = | 0.73(CSF46) | +0.46(CSF32) | +0.29(CSF36) | +··· | 3.657 |
| $\Psi$ ($3^2$A) = | 0.66(CSF44) | +0.36(CSF50) | +0.28(CSF34) | +0.26(CSF18) | |
| | +0.25(CSF52) | −0.20(CSF46) | +··· | | 5.060 |
| $\Psi$ ($4^2$A) = | 0.48(CSF18) | +0.47(CSF32) | −0.38(CSF46) | −0.31(CSF44) | |
| | −0.24(CSF50) | +··· | | | 5.155 |
| $\Psi$ ($5^2$A) = | 0.52(CSF24) | −0.49(CSF18) | −0.30(CSF39) | −0.30(CSF46) | |
| | +0.27(CSF32) | +0.22(CSF36) | +··· | | 5.515 |
| $\Psi$ ($6^2$A) = | −0.66(CSF24) | −0.32(CSF46) | +0.29(CSF36) | +0.23(CSF32) | |
| | −0.22(CSF18) | −0.21(CSF39) | +··· | | 5.649 |
| $\Psi$ ($7^2$A) = | −0.79(CSF23) | −0.29(CSF31) | −0.25(CSF43) | +··· | 6.285 |
| $\Psi$ ($8^2$A) = | −0.55(CSF43) | −0.50(CSF34) | +0.41(CSF33) | +0.30(CSF49) | |
| | −0.20(CSF51) | +··· | | | 6.474 |

tation angle are given in Fig. 4. The 7-th and 8-th solutions for $^4$A were so high in energy that they are not shown in the figure. The potential curve for each state rises monotonously along with an increase in the torsion angle. For the lower three states of $^4$A, the respective curves are very close to the corresponding ones for the lower three excited states of $^2$A. The TD-like CI wave functions and CSF's appearing in them are listed in Tables 3 and 4, respectively. The tables reveal that the first, second, and third quartet states arise from almost the same configuration as do the second, third, and fourth doublet states, respectively, showing a consistency with the results concerning the potential curves.

We recall that the energies of the irradiated UV were 3.52 and 4.89 eV. Considering the accuracy of the calculations and the irradiation energy of the experiment as well as taking account of the rather large energy gap between the 5-th and 6-th excited states of the respective symmetry, we discuss the characteristics of the five lowest excited states in detail.

The doublet states are discussed first. The first excited state lies 3.54 eV above the ground state. The main component (CSF46) expresses the excitation from the phenyl $\pi$-like orbital (40a) to the phenyl $\pi^*$-like orbital (45a). The CSF32 and CSF38 express the excitations from the phenyl $\pi$-like orbital of 38a to the carbonyl $\pi^*$-like orbital of 42a, and to the orbital of 49a consisting of $p_z$'s of C1, C4, and C7, respectively. The second excited state exists 4.83 eV above the ground state, and mainly comprises excitations of the phenyl $\pi$-like 40a to carbonyl $\pi^*$-like 42a (CSF44) and to $\pi^*$-like 49a discussed above (CSF52). The other three states are 5.01, 5.48, and 5.49 eV above the ground state; their characteristics are $\pi\rightarrow\pi^*$, $\pi\rightarrow\pi^*$, and $\sigma\rightarrow\pi^*$ excitations.

Table 3. (Continued)

| $^4$A states | | | | | $\Delta E$ (eV) $\{E-E(1^2\text{A } 0°)\}$[a] |
|---|---|---|---|---|---|
| Torsion angle 0° | | | | | |
| $\Psi$ ($1^4$A) = | 0.73(CSF3) | +0.50(CSF11) | +0.33(CSF16) | +··· | 3.571 |
| $\Psi$ ($2^4$A) = | −0.79(CSF2) | −0.49(CSF7) | −0.28(CSF12) | +··· | 4.910 |
| $\Psi$ ($3^4$A) = | 0.63(CSF11) | −0.56(CSF3) | +0.39(CSF43) | +0.20(CSF16) +··· | 5.109 |
| $\Psi$ ($4^4$A) = | −0.93(CSF48) | +0.24(CSF52) | +··· | | 5.687 |
| $\Psi$ ($5^4$A) = | 0.74(CSF43) | −0.45(CSF16) | +0.28(CSF3) | −0.21(CSF11) +··· | 5.826 |
| $\Psi$ ($6^4$A) = | 0.94(CSF12) | −0.26(CSF2) | +··· | | 6.475 |
| $\Psi$ ($7^4$A) = | −0.61(CSF23) | −0.52(CSF8) | +0.40(CSF7) | −0.27(CSF44) +··· | 8.093 |
| $\Psi$ ($8^4$A) = | 0.63(CSF22) | +0.44(CSF17) | +0.40(CSF27) | −0.26(CSF47) | |
| | −0.25(CSF16) | +··· | | | 8.180 |
| Torsion angle 15° | | | | | |
| $\Psi$ ($1^4$A) = | −0.73(CSF3) | +0.49(CSF11) | +0.32(CSF16) | +··· | 3.599 |
| $\Psi$ ($2^4$A) = | −0.77(CSF2) | −0.47(CSF7) | +0.29(CSF12) | +··· | 4.969 |
| $\Psi$ ($3^4$A) = | 0.62(CSF11) | +0.55(CSF3) | +0.40(CSF43) | +0.20(CSF16) +··· | 5.150 |
| $\Psi$ ($4^4$A) = | 0.90(CSF48) | −0.22(CSF52) | −0.22(CSF43) | +··· | 5.714 |
| $\Psi$ ($5^4$A) = | −0.70(CSF43) | −0.43(CSF16) | −0.28(CSF3) | −0.21(CSF48) | |
| | −0.21(CSF11) | +··· | | | 5.836 |
| $\Psi$ ($6^4$A) = | −0.93(CSF12) | −0.27(CSF2) | +··· | | 6.484 |
| $\Psi$ ($7^4$A) = | −0.54(CSF23) | +0.44(CSF8) | −0.36(CSF7) | −0.30(CSF31) | |
| | +0.28(CSF9) | −0.27(CSF44) | +··· | | 8.119 |
| $\Psi$ ($8^4$A) = | −0.55(CSF22) | −0.37(CSF17) | −0.33(CSF27) | −0.29(CSF30) | |
| | −0.25(CSF18) | +0.23(CSF47) | +0.23(CSF16) | −0.20(CSF35) +··· | 8.216 |
| Torsion angle 30° | | | | | |
| $\Psi$ ($1^4$A) = | 0.74(CSF3) | −0.45(CSF11) | −0.28(CSF15) | +··· | 3.681 |
| $\Psi$ ($2^4$A) = | 0.72(CSF2) | +0.42(CSF6) | −0.32(CSF12) | +0.29(CSF7) +··· | 5.134 |
| $\Psi$ ($3^4$A) = | 0.60(CSF11) | +0.51(CSF3) | +0.41(CSF43) | +··· | 5.270 |
| $\Psi$ ($4^4$A) = | 0.75(CSF48) | −0.49(CSF43) | +··· | | 5.777 |
| $\Psi$ ($5^4$A) = | −0.54(CSF43) | +0.37(CSF15) | +0.29(CSF3) | +0.25(CSF16) +··· | 5.872 |
| $\Psi$ ($6^4$A) = | 0.92(CSF12) | +0.29(CSF2) | +··· | | 6.520 |
| $\Psi$ ($7^4$A) = | 0.50(CSF23) | +0.48(CSF8) | −0.31(CSF31) | −0.27(CSF6) | |
| | −0.26(CSF38) | −0.25(CSF9) | +0.23(CSF44) | +··· | 8.199 |
| $\Psi$ ($8^4$A) = | −0.48(CSF22) | −0.41(CSF17) | −0.29(CSF30) | −0.26(CSF26) | |
| | −0.22(CSF37) | −0.22(CSF18) | +··· | | 8.320 |

a) Total energy of the ground state ($\Psi(1\ ^2\text{A } 0°)$) was −494.97914 a.u.

The lowest three excited states of $^4$A lie 3.57, 4.91, and 5.11 eV above the ground state; they are $\pi\rightarrow\pi^*$ transitions (as is $^2$A) and the characters of the $^4$A's are parallel to those corresponding to the $^2$A's. The 4-th and 5-th states are 5.69 and 5.83 eV above the ground state. Contrary to the doublet states, the lower is the $\sigma\rightarrow\pi^*$ transition and the higher is the $\pi\rightarrow\pi^*$ transition. Although we found the excited states in the preferable energy region, all states including the ground states have the minimum at a torsion angle of 0°.

**MCSCF-Like CI Calculation.** In TD-like CI calculations, only the deformation of the orbitals is considered for $^2$A, and the deformation of the orbitals and correlation effects are only partly taken account for $^4$A. We are afraid that an incomplete inclusion of the deformation of the orbitals and an insufficient inclusion of the correlation effects result in the incorrect potential energy curves mentioned above.

We therefore performed two types of fairly large CI calculations. One is called MCSCF-like CI calculations, which are discussed below.

Selecting 54 CSF's and 52 CSF's for the $^2$A and $^4$A states which have a weight larger than 1% at any angle in TD-like CI, we performed 1- and 2-electron excitation CI calculations with considerable limitations.

We recall that the SCF orbitals for a torsion angle of 0° were similar to those of 15° and 30°. In this CI, we paid attention mainly to the $\pi\rightarrow\pi^*$ like transition, and classified the orbitals into four categories:

a) Frozen orbitals: 1-24a orbitals having lower orbital energies than the first $\pi$-like orbital.

b) Valence orbitals: all occupied $\pi$-like orbitals in CSF's (25a, 29a, 32a, 36a, 38a, 39a, 40a, 42a, 45a, 47a, 49a, and 56a); two $\sigma$-like orbitals (48a and 57a), which were unoccupied in RHF configuration, but were occupied in the reference CSF's (54 CSF's for $^2$A and 52 for $^4$A); and four additional $\sigma$-like occupied orbitals, which were important in the C1, O2, O3, C4, and C15 area,

Table 4. Important Configurations in TD-Like CI Calculations[a,b]

| | | | | | | | | | |
|---|---|---|---|---|---|---|---|---|---|
| $^2$A states | | | | | | | | | |
| CSF1:[c] | $[(38a)^2]$ | (39a) | $(40a)^2$ | | CSF29,30: | (38a) | (39a) | (41a) | $(\pi\rightarrow\sigma)$ |
| CSF2,3:[d] | (25a) | (39a) | (42a) | $(\pi\rightarrow\pi)$ | CSF31,32:[c] | (38a) | (39a) | (42a) | $(\pi\rightarrow\pi)$ |
| CSF4,5: | (29a) | (39a) | (42a) | $(\pi\rightarrow\pi)$ | CSF33,34:[c] | (38a) | (39a) | (45a) | $(\pi\rightarrow\pi)$ |
| CSF6,7: | (32a) | (39a) | (42a) | $(\pi\rightarrow\pi)$ | CSF35,36:[c] | (38a) | (39a) | (48a) | $(\pi\rightarrow\sigma)$ |
| CSF8,9: | (32a) | (39a) | (56a) | $(\pi\rightarrow\pi)$ | CSF37,38:[c] | (38a) | (39a) | (49a) | $(\pi\rightarrow\pi)$ |
| CSF10,11: | (32a) | (39a) | (57a) | $(\pi\rightarrow\sigma)$ | CSF39:[c] | | $(39a)^2$[c] | (42a) | $(\pi\rightarrow\pi)$ |
| CSF12,13: | (33a) | (39a) | (42a) | $(\sigma\rightarrow\pi)$ | CSF40: | | $(39a)^2$ | (40a) | $(\pi\rightarrow\pi)$ |
| CSF14,15: | (34a) | (39a) | (42a) | $(\sigma\rightarrow\pi)$ | CSF41,42: | | (39a) | (40a) | (41a) $(\pi\rightarrow\sigma)$ |
| CSF16: | (36a) | $(39a)^2$ | | $(\pi\rightarrow\pi)$ | CSF43,44:[c] | | (39a) | (40a) | (42a) $(\pi\rightarrow\pi)$ |
| CSF17,18:[c] | (36a) | (39a) | (42a) | $(\pi\rightarrow\pi)$ | CSF45,46:[c] | | (39a) | (40a) | (45a) $(\pi\rightarrow\pi)$ |
| CSF19,20: | (36a) | (39a) | (48a) | $(\pi\rightarrow\sigma)$ | CSF47,48: | | (39a) | (40a) | (47a) $(\pi\rightarrow\pi)$ |
| CSF21,22: | (36a) | (39a) | (49a) | $(\pi\rightarrow\pi)$ | CSF49, 50:[c] | | (39a) | (40a) | (48a) $(\pi\rightarrow\sigma)$ |
| CSF23,24:[c] | (37a) | (39a) | (42a) | $(\sigma\rightarrow\pi)$ | CSF51,52:[c] | | (39a) | (40a) | (49a) $(\pi\rightarrow\pi)$ |
| CSF25,26: | (37a) | (39a) | (48a) | $(\sigma\rightarrow\sigma)$ | CSF53: | (38a) | $(39a)^2$ | | $(\pi\rightarrow\pi)$ |
| CSF27,28: | (37a) | (39a) | (49a) | $(\sigma\rightarrow\pi)$ | CSF54: | (37a) | $(39a)^2$ | | $(\sigma\rightarrow\pi)$ |
| $^4$A states | | | | | | | | | |
| CSF1: | | (39a) | (40a) | (41a) $(\pi\rightarrow\sigma)$ | | CSF27: | (32a) | (39a) | (49a) $(\pi\rightarrow\pi)$ |
| CSF2:[c] | | (39a) | (40a) | (42a) $(\pi\rightarrow\pi)$ | | CSF28: | (32a) | (39a) | (56a) $(\pi\rightarrow\pi)$ |
| CSF3:[c] | | (39a) | (40a) | (45a) $(\pi\rightarrow\pi)$ | | CSF29: | (32a) | (39a) | (57a) $(\pi\rightarrow\sigma)$ |
| CSF4: | | (39a) | (40a) | (46a) $(\pi\rightarrow\sigma)$ | | CSF30:[c] | (33a) | (39a) | (42a) $(\sigma\rightarrow\pi)$ |
| CSF5: | | (39a) | (40a) | (47a) $(\pi\rightarrow\pi)$ | | CSF31: | (33a) | (39a) | (45a) $(\sigma\rightarrow\pi)$ |
| CSF6:[c] | | (39a) | (40a) | (48a) $(\pi\rightarrow\sigma)$ | | CSF32: | (33a) | (39a) | (46a) $(\sigma\rightarrow\sigma)$ |
| CSF7:[c] | | (39a) | (40a) | (49a) $(\pi\rightarrow\pi)$ | | CSF33: | (33a) | (39a) | (47a) $(\sigma\rightarrow\pi)$ |
| CSF8: | | (39a) | (40a) | (56a) $(\pi\rightarrow\pi)$ | | CSF34: | (33a) | (39a) | (48a) $(\sigma\rightarrow\sigma)$ |
| CSF9: | | (39a) | (40a) | (57a) $(\pi\rightarrow\sigma)$ | | CSF35: | (33a) | (39a) | (49a) $(\sigma\rightarrow\pi)$ |
| CSF10: | (38a) | (39a) | (41a) | $(\pi\rightarrow\sigma)$ | | CSF36: | (33a) | (39a) | (56a) $(\sigma\rightarrow\pi)$ |
| CSF11:[c] | (38a) | (39a) | (42a) | $(\pi\rightarrow\pi)$ | | CSF37: | (34a) | (39a) | (42a) $(\sigma\rightarrow\pi)$ |
| CSF12:[c] | (38a) | (39a) | (45a) | $(\pi\rightarrow\pi)$ | | CSF38: | (34a) | (39a) | (45a) $(\sigma\rightarrow\pi)$ |
| CSF13: | (38a) | (39a) | (46a) | $(\pi\rightarrow\sigma)$ | | CSF39: | (34a) | (39a) | (46a) $(\sigma\rightarrow\sigma)$ |
| CSF14: | (38a) | (39a) | (47a) | $(\pi\rightarrow\pi)$ | | CSF40: | (34a) | (39a) | (47a) $(\sigma\rightarrow\pi)$ |
| CSF15:[c] | (38a) | (39a) | (48a) | $(\pi\rightarrow\sigma)$ | | CSF41: | (34a) | (39a) | (48a) $(\sigma\rightarrow\sigma)$ |
| CSF16:[c] | (38a) | (39a) | (49a) | $(\pi\rightarrow\pi)$ | | CSF42: | (34a) | (39a) | (49a) $(\sigma\rightarrow\pi)$ |
| CSF17: | (38a) | (39a) | (56a) | $(\pi\rightarrow\pi)$ | | CSF43:[c] | (36a) | (39a) | (42a) $(\pi\rightarrow\pi)$ |
| CSF18: | (38a) | (39a) | (57a) | $(\pi\rightarrow\sigma)$ | | CSF44: | (36a) | (39a) | (45a) $(\pi\rightarrow\pi)$ |
| CSF19: | (25a) | (39a) | (42a) | $(\pi\rightarrow\pi)$ | | CSF45: | (36a) | (39a) | (46a) $(\pi\rightarrow\sigma)$ |
| CSF20: | (29a) | (39a) | (42a) | $(\pi\rightarrow\pi)$ | | CSF46: | (36a) | (39a) | (48a) $(\pi\rightarrow\sigma)$ |
| CSF21: | (30a) | (39a) | (42a) | $(\sigma\rightarrow\pi)$ | | CSF47: | (36a) | (39a) | (49a) $(\pi\rightarrow\pi)$ |
| CSF22: | (32a) | (39a) | (42a) | $(\pi\rightarrow\pi)$ | | CSF48:[c] | (37a) | (39a) | (42a) $(\sigma\rightarrow\pi)$ |
| CSF23: | (32a) | (39a) | (45a) | $(\pi\rightarrow\pi)$ | | CSF49: | (37a) | (39a) | (45a) $(\sigma\rightarrow\pi)$ |
| CSF24: | (32a) | (39a) | (46a) | $(\pi\rightarrow\sigma)$ | | CSF50: | (37a) | (39a) | (46a) $(\sigma\rightarrow\sigma)$ |
| CSF25: | (32a) | (39a) | (47a) | $(\pi\rightarrow\pi)$ | | CSF51: | (37a) | (39a) | (48a) $(\sigma\rightarrow\sigma)$ |
| CSF26: | (32a) | (39a) | (48a) | $(\pi\rightarrow\sigma)$ | | CSF52: | (37a) | (39a) | (49a) $(\sigma\rightarrow\pi)$ |

a) All the CSF's listed in this Table were treated as the reference CSF's in the MCSCF-like CI calculations. b) Only the singly occupied orbitals and 39th orbital were presented except for CSF1 of $^2$A state. c) These CSF's are treated as reference CSF's in a large SDMR-CI calculation. d) Two spin configurations are possible for the $^2$A state which has three singly occupied orbitals; $(\alpha\beta\alpha)-(\alpha\alpha\beta)$ and $(\alpha\beta\alpha)+(\alpha\alpha\beta)-2(\beta\alpha\alpha)$. Spin configuration for $^4$A is $(\alpha\alpha\alpha)$.

and whose orbital energies were not very deep, namely, shallower than −0.52 a.u. They were 33a, 34a, 37a, and 41a. Hereafter, we denote the valence orbitals as v, v′, v″, or v‴.

c) Semi-valence orbitals: all of the orbitals between 25a—99a, except for the orbitals included in b). The orbitals had orbital energies of between −0.65 and 1.01 a.u. We denote the semi-valence orbitals as either s or s′.

d) Higher orbitals: the remaining orbitals of 100a—117a.

All excitations from frozen orbitals were forbidden. The single excitation of (v→v′), (v→s), and (s→v) and the double excitation of (vv′→v″v‴), (vv′→v″s), and (vs→v′v″) were allowed. All excitations to higher orbitals were forbidden. Since the excitations among the π-like valence orbitals and the reorganization effects were taken into account, we call this CI MCSCF-like

Table 5. Wave Functions of MCSCF-Like CI Calculations

| $^2$A states | Weight of references (%) | $\Delta E$ (eV) $\{E-E(1^2\text{A } 0°)\}$[a] |
|---|---|---|
| Torsion angle 0° | | |
| $\Psi$ ($1^2$A) = 0.94(CSF1) +··· | 89.0 | 0.000 |
| $\Psi$ ($2^2$A) = −0.69(CSF46) +0.44(CSF31) +0.28(CSF37) +0.25(CSF32) +··· | 89.6 | 4.625 |
| $\Psi$ ($3^2$A) = −0.61(CSF44) −0.35(CSF52) −0.30(CSF39) +0.27(CSF33) +0.23(CSF34) −0.22(CSF17) +··· | 87.8 | 5.613 |
| $\Psi$ ($4^2$A) = −0.57(CSF46) −0.51(CSF31) −0.28(CSF32) −0.25(CSF37) +··· | 86.0 | 5.698 |
| $\Psi$ ($5^2$A) = −0.48(CSF39) −0.43(CSF43) −0.37(CSF34) −0.26(CSF17) −0.26(CSF51) −0.21(CSF18) +··· | 84.8 | 5.770 |
| $\Psi$ ($6^2$A) = −0.43(CSF43) +0.41(CSF39) +0.35(CSF33) +0.27(CSF44) +0.26(CSF17) +0.20(CSF18) +··· | 85.0 | 5.836 |
| $\Psi$ ($7^2$A) = 0.82(CSF23) +0.34(CSF54) +0.21(CSF24) +··· | 86.7 | 6.111 |
| $\Psi$ ($8^2$A) = 0.87(CSF24) +··· | 85.8 | 6.560 |
| Torsion angle 15° | | |
| $\Psi$ ($1^2$A) = 0.95(CSF1) +··· | 89.6 | 0.276 |
| $\Psi$ ($2^2$A) = −0.72(CSF46) −0.42(CSF31) −0.26(CSF37) −0.23(CSF32) +··· | 89.7 | 4.971 |
| $\Psi$ ($3^2$A) = 0.57(CSF44) −0.35(CSF46) +0.31(CSF52) +0.26(CSF31) −0.17(CSF17) +0.14(CSF32) +··· | 88.4 | 6.021 |
| $\Psi$ ($4^2$A) = 0.47(CSF31) −0.45(CSF46) −0.34(CSF44) +0.25(CSF32) +0.24(CSF37) −0.21(CSF34) −0.21(CSF52) +··· | 87.0 | 6.076 |
| $\Psi$ ($5^2$A) = 0.58(CSF43) −0.41(CSF34) +0.34(CSF51) +0.31(CSF33) +··· | 83.2 | 6.162 |
| $\Psi$ ($6^2$A) = −0.66(CSF39) −0.39(CSF17) −0.31(CSF18) +··· | 88.4 | 6.265 |
| $\Psi$ ($7^2$A) = 0.81(CSF23) +0.33(CSF54) +··· | 87.3 | 6.419 |
| $\Psi$ ($8^2$A) = −0.88(CSF24) +··· | 86.3 | 6.813 |
| Torsion angle 30° | | |
| $\Psi$ ($1^2$A) = 0.95(CSF1) +··· | 89.8 | 0.441 |
| $\Psi$ ($2^2$A) = +0.75(CSF46) +0.36(CSF31) +0.22(CSF35) +0.21(CSF32) +··· | 89.3 | 5.233 |
| $\Psi$ ($3^2$A) = 0.50(CSF46) −0.48(CSF31) −0.28(CSF44) −0.25(CSF32) −0.23(CSF23) +··· | 87.9 | 6.322 |
| $\Psi$ ($4^2$A) = 0.47(CSF44) +0.45(CSF34) +0.34(CSF50) −0.25(CSF31) +0.24(CSF33) +0.21(CSF52) +··· | 88.5 | 6.407 |
| $\Psi$ ($5^2$A) = −0.56(CSF43) +0.39(CSF34) −0.38(CSF33) −0.30(CSF49) −0.21(CSF44) −0.20(CSF51) +··· | 84.2 | 6.493 |
| $\Psi$ ($6^2$A) = 0.68(CSF39) −0.45(CSF17) −0.33(CSF18) +··· | 89.1 | 6.753 |
| $\Psi$ ($7^2$A) = 0.78(CSF23) +0.33(CSF54) +··· | 87.5 | 6.770 |
| $\Psi$ ($8^2$A) = −0.87(CSF24) +··· | 86.7 | 7.089 |

CI.

The dimensions of the CI calculations were 163495 and 202802 for $^2$A and $^4$A, respectively; we performed a perturbation selection with a threshold value of 0.00001 a.u. The resulting CI dimensions were 5277 and 5318 for $^2$A and $^4$A, respectively. The total energies given by the SCF and MCSCF-like CI calculations for the ground state at a torsion angle of 0° were −494.96979 and −495.08300 a.u., respectively. The calculated correlation energy was rather small (3.08 eV). This probably arose from the fact that we were mainly concerned with $\pi$-like electrons, for which the electronic correlation effect is difficult to calculate, because of their diffuseness; thus, the near-degeneracy effect, ($\sigma\sigma\rightarrow\pi\pi$) and ($\sigma\sigma\rightarrow p_\sigma p_\sigma$), was almost disregarded. Furthermore, the CI space for $\pi$-like electrons was very limited (as shown above).

The potential curves are given in Fig. 5. The 6—8th solutions of the $^4$A state are excluded from this figure, because of their high excitation energies. Although the absolute value of the excitation energies and curvature were different from those of the TD-like CI, the profile resembles that of TD-like CI result, on the whole. The potential energy of each state rises monotonously, along with an increase in the torsion angle.

The obtained wave functions and potential energies relative to that of the first $^2$A state at a torsion angle 0° are summarized in Table 5.

Comparing the obtained wave functions at a torsion angle of 0° with those obtained by a TD-like CI calculation, we found that the first, second, and third $^2$A states of the MCSCF-like calculations are descendants of those in the TD-like CI calculation, even though the excitation energies arise nearly at 1 eV, compared with those of the TD-like CI. The seventh and eighth $^2$A states, which are the $\sigma\rightarrow\pi^*$ like excited stated, corre-

Table 5. (Continued)

| $^4$A states | | | | | | Weight of references (%) | $\Delta E$ (eV) $\{E-E(1^2\text{A } 0°)\}$[a] |
|---|---|---|---|---|---|---|---|
| Torsion angle 0° | | | | | | | |
| $\Psi$ ($1^4$A) = | 0.70(CSF3) | +0.50(CSF11) | +0.31(CSF16) | +··· | | 89.4 | 4.542 |
| $\Psi$ ($2^4$A) = | −0.66(CSF2) | −0.43(CSF12) | −0.39(CSF7) | −0.23(CSF3) | +··· | 86.9 | 5.481 |
| $\Psi$ ($3^4$A) = | 0.60(CSF11) | −0.55(CSF3) | +0.28(CSF16) | +··· | | 85.9 | 5.575 |
| $\Psi$ ($4^4$A) = | 0.90(CSF48) | +··· | | | | 87.4 | 6.202 |
| $\Psi$ ($5^4$A) = | −0.82(CSF43) | +0.35(CSF16) | +··· | | | 88.5 | 6.605 |
| $\Psi$ ($6^4$A) = | 0.79(CSF12) | −0.47(CSF2) | +··· | | | 91.3 | 7.469 |
| $\Psi$ ($7^4$A) = | −0.54(CSF23) | −0.43(CSF8) | +0.37(CSF7) | −0.28(CSF44) | +··· | 74.1 | 8.284 |
| $\Psi$ ($8^4$A) = | 0.61(CSF22) | +0.37(CSF17) | +0.34(CSF27) | −0.24(CSF16) | | | |
| | +0.21(CSF47) | +··· | | | | 75.6 | 8.377 |
| Torsion angle 15° | | | | | | | |
| $\Psi$ ($1^4$A) = | 0.73(CSF3) | −0.47(CSF11) | −0.29(CSF16) | +··· | | 90.0 | 4.858 |
| $\Psi$ ($2^4$A) = | 0.66(CSF2) | −0.44(CSF12) | +0.37(CSF7) | −0.23(CSF3) | +··· | 87.9 | 5.941 |
| $\Psi$ ($3^4$A) = | 0.61(CSF11) | +0.52(CSF3) | +0.28(CSF16) | +0.21(CSF2) | +··· | 87.1 | 5.942 |
| $\Psi$ ($4^4$A) = | 0.90(CSF48) | +··· | | | | 88.0 | 6.466 |
| $\Psi$ ($5^4$A) = | −0.82(CSF43) | −0.34(CSF16) | +··· | | | 89.2 | 6.986 |
| $\Psi$ ($6^4$A) = | 0.80(CSF12) | −0.47(CSF2) | +··· | | | 92.5 | 7.743 |
| $\Psi$ ($7^4$A) = | 0.50(CSF23) | −0.38(CSF8) | +0.36(CSF7) | −0.27(CSF44) | | | |
| | +0.26(CSF32) | −0.23(CSF9) | +··· | | | 76.5 | 8.788 |
| $\Psi$ ($8^4$A) = | −0.55(CSF22) | −0.32(CSF17) | −0.30(CSF27) | −0.27(CSF30) | | | |
| | +0.22(CSF16) | −0.21(CSF18) | +0.20(CSF47) | +··· | | 76.9 | 8.887 |
| Torsion angle 30° | | | | | | | |
| $\Psi$ ($1^4$A) = | −0.77(CSF3) | +0.41(CSF11) | +0.25(CSF15) | +··· | | 90.2 | 5.114 |
| $\Psi$ ($2^4$A) = | 0.61(CSF2) | −0.47(CSF12) | +0.33(CSF6) | −0.23(CSF7) | +··· | 88.5 | 6.152 |
| $\Psi$ ($3^4$A) = | 0.61(CSF11) | +0.47(CSF3) | +0.27(CSF15) | +··· | | 88.0 | 6.259 |
| $\Psi$ ($4^4$A) = | 0.87(CSF48) | +··· | | | | 88.3 | 6.779 |
| $\Psi$ ($5^4$A) = | −0.82(CSF43) | +0.34(CSF15) | +··· | | | 89.5 | 7.251 |
| $\Psi$ ($6^4$A) = | −0.78(CSF12) | −0.49(CSF2) | +··· | | | 93.2 | 7.798 |
| $\Psi$ ($7^4$A) = | 0.46(CSF23) | +0.42(CSF8) | +0.29(CSF31) | +0.27(CSF6) | | | |
| | +0.24(CSF44) | −0.23(CSF38) | −0.21(CSF9) | +··· | | 77.3 | 9.033 |
| $\Psi$ ($8^4$A) = | 0.47(CSF22) | −0.36(CSF17) | +0.27(CSF30) | +0.24(CSF26) | | | |
| | −0.21(CSF37) | +··· | | | | 76.5 | 9.182 |

a) Total energy of the ground state ($\Psi(1^2\text{A } 0°)$) was −495.08300 a.u.

spond to the seventh and sixth $^2$A states in the TD-like CI calculation, respectively.

For the $^4$A states, the respective wave functions of the MCSCF-like CI calculations in due order maintain almost the same character as do those of the TD-like CI calculations.

**Large SDMR-CI Calculation.** We are further afraid that we disregarded such correlation effects as ($\pi\pi\rightarrow\sigma^*\sigma^*$); we therefore intended to perform a larger SDMR-CI calculation.

Since the resources were, however, limited, restrictions were imposed on a number of the reference functions. We chose CSF's from the MCSCF-like CI calculation which had weights larger than 0.09 (9%) at any torsion angle. The number of selected CSF's were 22 and 11 for $^2$A and $^4$A, respectively (indicated by c in Table 4). The orbitals are classified into the following three categories; it will soon be shown that the number of valence orbitals is considerably increased compared to the case of the MCSCF-like CI calculation:

a) Frozen orbitals (1—21a), whose orbital energy is deeper than −0.75 a.u.

b) Valence orbitals (v, v′, v″, and v‴): all of the doubly and singly occupied $\sigma$- and $\pi$-like orbitals which have orbital energies higher than −0.75 a.u. (7 $\pi$-like and 12 $\sigma$-like SCF orbitals), the virtual orbitals appearing in reference CSF's (3 $\pi$-like and 1 $\sigma$-like orbitals), $\pi$-like orbitals having orbital energies less than 0.71 a.u. (9 $\pi$-like orbitals), and 9 $\sigma$-like orbitals which satisfy the following conditions: i) orbital energies were less than 0.75 a.u. and ii) the sum of occupation numbers at C1 and C4 was larger than 0.4 or occupation number either C1 or C4 is larger than 0.3. Totally, 19 $\pi$-like and 22 $\sigma$-like orbitals are treated as valence orbitals.

c) Semi-valence orbitals (s): the remaining 55 orbitals.

Single excitations of (v→v′) and (v→s) and double excitation of (vv′→v″v‴) from the reference CSF's are allowed. Since the 9 unoccupied $\sigma$-like orbitals in the valence orbital space had a relatively larger amplitude

Table 6. Wave Functions of Large SDMR-CI Calculations

| | | | | | | Weight of references (%) | $\Delta E$ (eV) $\{E-E(1^2A\ 0°)\}$[a] |
|---|---|---|---|---|---|---|---|
| | | $^2A$ states | | | | | |
| Torsion angle 0° | | | | | | | |
| $\Psi$ ($1^2A$) | = | 0.93(CSF1) | +··· | | | 88.5 | 0.000 |
| $\Psi$ ($2^2A$) | = | 0.76(CSF46) | +0.39(CSF31) | +0.22(CSF37) | −0.21(CSF32) +··· | 86.6 | 5.467 |
| $\Psi$ ($3^2A$) | = | 0.68(CSF39) | +0.35(CSF44) | +0.34(CSF17) | +0.27(CSF18) +··· | 83.5 | 6.192 |
| $\Psi$ ($4^2A$) | = | 0.77(CSF23) | +0.48(CSF24) | +··· | | 81.6 | 6.226 |
| $\Psi$ ($5^2A$) | = | −0.60(CSF44) | +0.37(CSF39) | +0.32(CSF52) | +0.30(CSF46) | | |
| | | +0.22(CSF34) | +··· | | | 85.5 | 6.395 |
| $\Psi$ ($6^2A$) | = | 0.56(CSF31) | +0.43(CSF46) | +0.29(CSF32) | +0.28(CSF44) | | |
| | | −0.25(CSF37) | +··· | | | 84.7 | 6.460 |
| Torsion angle 15° | | | | | | | |
| $\Psi$ ($1^2A$) | = | −0.94(CSF1) | +··· | | | 89.1 | 0.487 |
| $\Psi$ ($2^2A$) | = | 0.77(CSF46) | +0.37(CSF31) | +0.21(CSF37) | −0.21(CSF32) +··· | 87.0 | 5.995 |
| $\Psi$ ($3^2A$) | = | −0.66(CSF39) | −0.32(CSF17) | +0.25(CSF44) | −0.27(CSF23) | | |
| | | −0.25(CSF18) | +··· | | | 83.2 | 6.691 |
| $\Psi$ ($4^2A$) | = | −0.62(CSF23) | −0.46(CSF24) | +0.35(CSF39) | +··· | 82.4 | 6.753 |
| $\Psi$ ($5^2A$) | = | −0.66(CSF44) | −0.35(CSF52) | −0.28(CSF22) | −0.25(CSF34) | | |
| | | −0.22(CSF39) | −0.20(CSF33) | +··· | | 85.8 | 6.943 |
| $\Psi$ ($6^2A$) | = | −0.67(CSF24) | +0.51(CSF23) | +··· | | 82.0 | 6.989 |
| | | $^4A$ states | | | | | |
| Torsion angle 0° | | | | | | | |
| $\Psi$ ($1^4A$) | = | 0.66(CSF3) | +0.54(CSF11) | −0.30(CSF16) | +··· | 87.0 | 5.294 |
| $\Psi$ ($2^4A$) | = | 0.72(CSF2) | +0.41(CSF12) | −0.39(CSF7) | +··· | 87.0 | 5.926 |
| $\Psi$ ($3^4A$) | = | −0.91(CSF48) | +··· | | | 85.0 | 6.097 |
| $\Psi$ ($4^4A$) | = | 0.62(CSF3) | −0.56(CSF11) | +0.24(CSF16) | +0.24(CSF43) +··· | 85.8 | 6.150 |
| $\Psi$ ($5^4A$) | = | 0.82(CSF43) | −0.38(CSF16) | +··· | | 84.2 | 7.107 |
| $\Psi$ ($6^4A$) | = | 0.83(CSF12) | −0.43(CSF2) | +··· | | 89.6 | 7.690 |
| Torsion angle 15° | | | | | | | |
| $\Psi$ ($1^4A$) | = | −0.69(CSF3) | +0.52(CSF11) | +0.28(CSF16) | +··· | 87.2 | 5.830 |
| $\Psi$ ($2^4A$) | = | −0.67(CSF2) | +0.39(CSF12) | −0.34(CSF7) | −0.29(CSF48) | | |
| | | +0.23(CSF3) | +··· | | | 86.9 | 6.479 |
| $\Psi$ ($3^4A$) | = | −0.78(CSF48) | +0.26(CSF2) | +0.22(CSF3) | +0.22(CSF11) +··· | 85.1 | 6.606 |
| $\Psi$ ($4^4A$) | = | −0.56(CSF11) | −0.53(CSF1) | −0.36(CSF48) | −0.23(CSF16) | | |
| | | +0.27(CSF43) | +··· | | | 85.9 | 6.751 |
| $\Psi$ ($5^4A$) | = | 0.82(CSF43) | −0.38(CSF16) | +··· | | 83.8 | 7.656 |
| $\Psi$ ($6^4A$) | = | 0.83(CSF12) | −0.43(CSF2) | +··· | | 90.2 | 8.221 |

a) Total energy of the ground state ($\Psi(1^2A\ 0°)$) was −495.14247 a.u.

in the region of C1 and C4, we thus paid much attention to the movement of the electrons in the "neck area".

This CI calculation was performed for torsion angles of 0° and 15°. The numbers of the CI dimension were 2006186 and 1083959 for the $^2A$ and $^4A$ states, respectively. We have decreased the number of dimensions by perturbation selection. The threshould of 0.0001 a.u. reduced the CI dimensions of $^2A$ to 16046 and those of $^4A$ to 12503.

The total energy for the ground state at a torsion angle of 0° was −495.14247 a.u., resulting in a correlation energy of 4.70 eV, which was 50% greater than that of an MCSCF-like CI calculation.

The potential-energy curves up to the sixth solution for each symmetry are shown in Fig. 6. The energy differences between the lowest $^2A$ having a torsion angle of 0° and the respective states of 0° and 15° are given in Table 6 together with the wave functions.

We can see from Fig. 6 that all of the potential energies having a torsion angle of 15° are higher than those having a torsion angle of 0°. The slopes become steeper than those of the MCSCF-like calculations. The correlation effects make the states having a torsion angle of 0° more stable.

The table shows that the lower two excited states of the large CI calculations are $\pi\rightarrow\pi^*$ like in both $^2A$ and $^4A$. Comparing the wave functions in Tables 5 and 6, one may find that the characteristics of the lowest excited states in the respective symmetries are parallel to those of the MCSCF-like ones. In contrast to the MCSCF-like calculations, the third excited states are $\sigma\rightarrow\pi^*$ like, suggesting that the correlation effects are

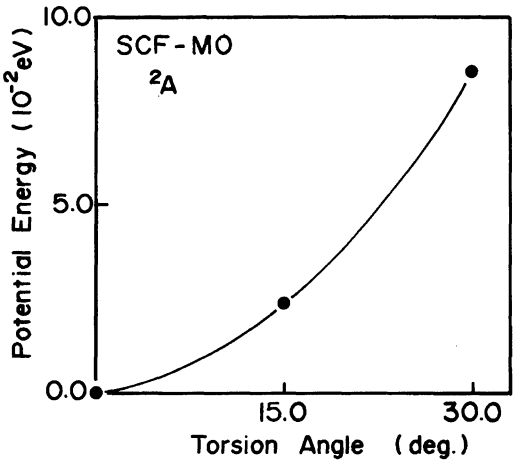


Fig. 3. Potential energy change of the SCF $^2$A ground state.

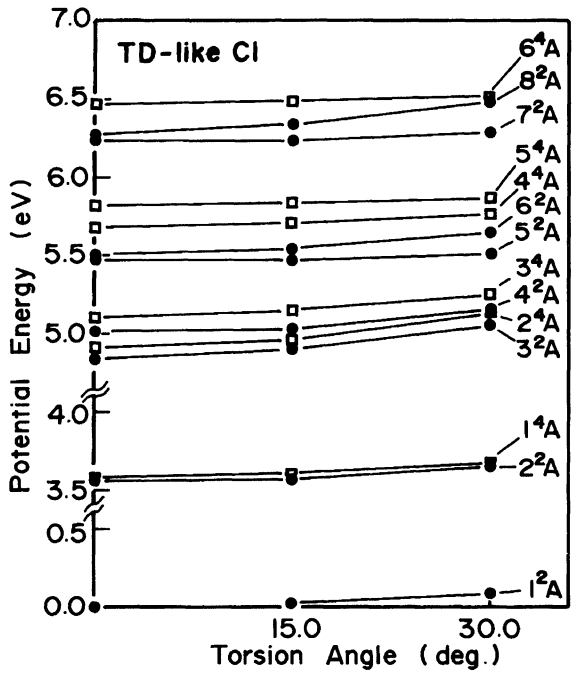


Fig. 4. Potential energy changes of the $^2$A and $^4$A states obtained by TD-like CI calculations.

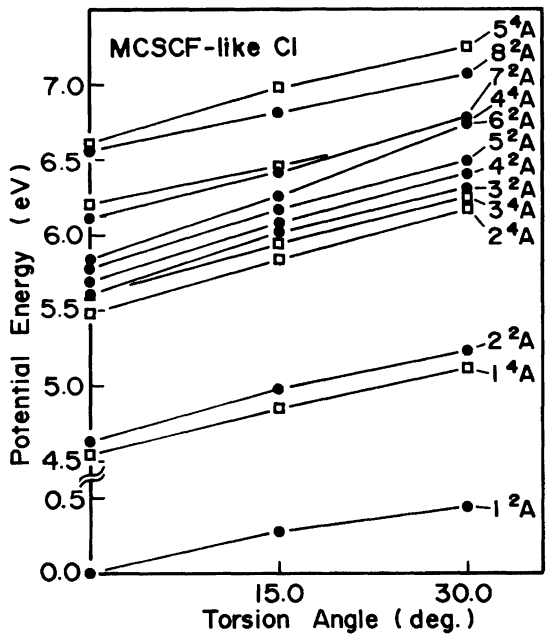


Fig. 5. Potential energy changes of the $^2$A and $^4$A states obtained by MCSCF-like CI calculations.

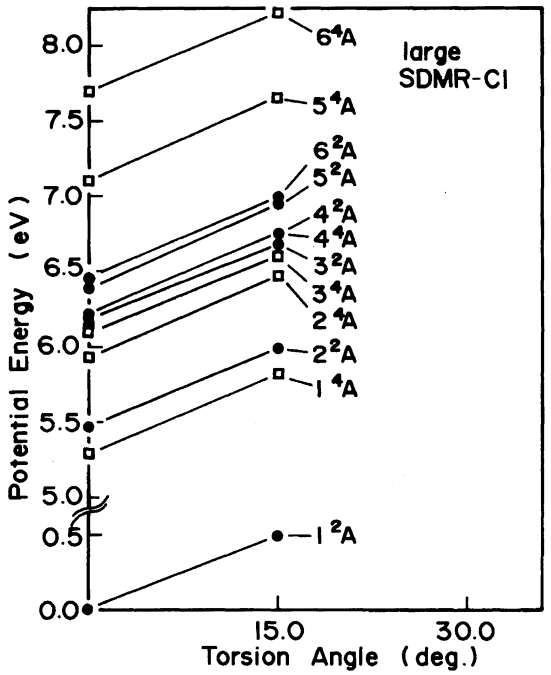


Fig. 6. Potential energy changes of the $^2$A and $^4$A states obtained by large SDMR-CI calculations.

important for this type of excitation.

The excitation energies given by the large SDMR-CI calculations were slightly larger than those of the MC-SCF-like calculations. In this calculation, the ground-state SCF-MO was used not only for the ground-state CI calculation, but also for calculations of the other states. The magnitude of the correlation effects taken into account for the ground-state was larger than for the other states, and the resulting excitation energies became larger. The present CI calculation cannot correct the results of the MCSCF-like calculation, although we have tried to recover the correlation effects disregarded in the MCSCF-like calculations, by extending the CI space. The threshold taken into account was 0.0001 a.u.; this was probably large for proper estimations of the correlation energies as well as proper corrections concerning the shape of the orbitals for the excited states. The natural orbital iterations for the respective states were desirable, but not performed in the present calculations.

We, however, feel that the conclusions concerning the positions of the minimum potential given by the large

SDMR-CI hardly changes, even if such investigations were performed, since the potential curves by the large SDMR-CI, were very steep compared with the MCSCF-like CI, as discussed above.

## Concluding Remarks

We have investigated the geometrical structure of $CH_3\dot{C}HOCOC_6H_5$ in relation to the stereochemistry of the polymerization of vinyl benzoate (we replace the polymer with $CH_3\dot{C}HOCOC_6H_5$). We have changed the torsion angle between the phenyl and carbonyl groups. Within the examined torsion range, it was shown that a planar structure is the most stable for both the ground and excited states of the model molecule. The possibility of a transformation to a less isotactic species by internal conversion was negated from the profile of the potential curves, so long as we considered the mono-molecular process using this model.

Although the absorption spectra during the polymerization reaction has not been observed, it was experimentally confirmed that UV irradiation had an apparent effect on the stereoregularity of PVA. In this synthesis, the starting material, i.e., vinyl benzoate, itself, was a solvent. The present calculations were performed for a model molecule in an isolated state instead of a polymer in a solvent. Investigations concerning the dimer-like radical of the present model, $CH_3CH(OCOC_6H_5)$-$CH_2\dot{C}H(OCOC_6H_5)$, are highly desirable, by which the very early stage of polymerization and the influence of remaining parts of the polymer are expected to be clarified.

All of the computations were carried out on an NEC ACOS 930-10 at the Computation Center of Nagoya City University.

The present research was partly supported by a Grant-in-Aid for Scientific Research on Priority Area 'Theory of Chemical Reactions' from the Ministry of Education, Science and Culture.

## References

1) K. Imai and M. Matsumoto, *Kobunshi Ronbunshu*, **35**, 743 (1978).
2) K. Imai, T. Shiomi, N. Oda, and H. Otsuka, *J. Polym. Sci.*, **24**, 3225 (1986).
3) K. Imai and M. Matsumoto, "9th Polym. Symp. Jpn.," Preprints p. 217 (1960).
4) S. Nozakura, M. Sumi, M. Uoi, T. Okamoto, and S. Murahashi, *J. Polym. Sci., Polym. Chem. Ed.*, **11**, 279 (1973).
5) S. Nozakura, T. Okamoto, K. Toyoura, and S. Murahashi, *J. Polym. Sci., Polym. Chem. Ed.*, **11**, 1043 (1973).
6) K. Imai, T. Shiomi, Y. Tezuka, T. Kawanishi, and T. Jin, *J. Polym. Sci., Polym. Chem. Ed.*, **26**, 1961 (1988).
7) K. Imai, T. Shiomi, Y. Tezuka, N. Fujioka, T. Hosokawa, N. Ueda, and K. Fujita, *Kobunshi Ronbunshu*, **46**, 261 (1989).
8) K. Imai, T. Shiomi, Y. Tezuka, N. Uchida, M. Oura, and K. Fujita, *Polymer, Preprints (Jpn.)*, **39**, 1433 (1990).
9) "Tables of Interatomic Distances and Configuration in Molecules and Ions, Special Publication No. 11," ed by L. E. Sutton, The Chemical Society, London (1958).
10) H. Tatewaki and S. Huzinaga, *J. Comput. Chem.*, **1**, 205 (1980).